Brain Stimulation 12 (2019) 743–751

Contents lists available at ScienceDirect

Brain Stimulation

journal homepage: http://www.journals.elsevier.com/brain-stimulation

Autonomic arousal elicited by subcallosal cingulate stimulation is explained by white matter connectivity

Patricio Riva-Posse [a, *, 1], Cory S. Inman [b, c, 1], Ki Sueng Choi [f], Andrea L. Crowell [a], Robert E. Gross [b, d, e], Stephan Hamann [c], Helen S. Mayberg [a, f]

[a] Department of Psychiatry and Behavioral Sciences, Emory University School of Medicine, 101 Woodruff Circle, Atlanta, 30322, GA, USA
[b] Department of Neurosurgery, Emory University School of Medicine, 1365 Clifton Road, Atlanta, 30322, GA, USA
[c] Department of Psychology, Emory University, 36 Eagle Row, Atlanta, 30322, GA, USA
[d] Department of Neurology, Emory University School of Medicine, 1365 Clifton Road, Atlanta, 30322, GA, USA
[e] Coulter Department of Biomedical Engineering, Georgia Institute of Technology & Emory University School of Medicine, 1760 Haygood Dr., Atlanta, 30322, GA, USA
[f] Department of Psychiatry, Icahn School of Medicine at Mount Sinai, 1470 Madison Ave, New York, 10029, NY, USA

ARTICLE INFO

Article history:
Received 5 February 2018
Received in revised form
11 December 2018
Accepted 22 January 2019
Available online 26 January 2019

Keywords:
Deep brain stimulation
Depression
Subcallosal cingulate
Sympathetic activity
Autonomic nervous system

ABSTRACT

Background: Subcallosal cingulate deep brain stimulation (SCC DBS) is an experimental treatment for severe depression. Surgery is performed with awake patients and intraoperative stimulation produces acute behavioral responses in select contacts. While there have been reports on the relationship between acute intraoperative behaviors and their relation to the location of the contacts, there are no descriptions of the physiological changes that accompany them.
Objective: The present study sought to examine these physiological readouts, and their association with the anatomical substrates that generated them.
Methods: Nine patients with severe, treatment-resistant depression were tested intraoperatively. The stimulation protocol consisted of 12 three-minute, sham-controlled, double-blind trials. Changes in heart rate and skin conductance were recorded during each stimulation cycle. Probabilistic tractography between the stimulated contacts and predefined regions of the mood regulation network was performed.
Results: Acute intraoperative SCC stimulation produced increases in autonomic sympathetic response that correlated with the salience of the behavioral responses. The autonomic changes were observed within seconds of initiating acute stimulation and prior to verbalization of subjective experiences. The probabilistic tractography analysis suggested that structural connectivity between the stimulated area and the midcingulate cortex is the primary pathway that mediates autonomic responsivity to SCC DBS.
Conclusions: These findings demonstrate that acute SCC stimulation produces autonomic and behavioral changes in the operating room that are explained by the modulation of networks associated with long term antidepressant response. Intraoperative autonomic recordings paired with careful behavioral observations and precise anatomical mapping aid in the identification and classification of the intraoperative phenomena.

Introduction

Specific neural circuits within the limbic-cortical system mediate various aspects of mood and emotional regulation [1]. Deep brain stimulation (DBS) delivers electrical stimulation to neural circuits in a precise and controlled manner. Several DBS targets are being investigated for the treatment of mood disorders [2–4]. The most reported target for depression is the subcallosal cingulate white matter (SCC) [5]. Research suggests that the antidepressant response to SCC DBS is seen when a necessary group of

---

[*] Corresponding author. Department of Psychiatry and Behavioral Sciences, Emory University School of Medicine, 101 Woodruff Cir NE, Suite 4309, Atlanta, GA, 30322, USA.
E-mail address: privapo@emory.edu (P. Riva-Posse).

[1] Authors contributed equally to this manuscript.

https://doi.org/10.1016/j.brs.2019.01.015
1935-861X/

white matter bundles are impacted by the stimulation, and responders share a common tractography map [6]. This electrical stimulation impacts fibers that connect the SCC area to other regions, such as the medial frontal cortices bilaterally, dorsal and midcingulate cortices, and other subcortical regions, via the forceps minor, cingulum bundle and uncinate fasciculus. Using these tracts as a “blueprint” for targeting makes the therapeutic response to DBS more consistent [7].

The presurgical identification of the intended target also makes the acute response to stimulation more predictable and reproducible [8]. DBS surgery is usually performed with awake patients to evaluate the acute manifestations of the stimulation. These acute effects assist in the identification of optimal lead placement, side effects, and ideal stimulation parameters. Objective physiologic readouts of these stimulation effects have been identified in movement disorder DBS surgery, such as the beta oscillations of the cortico-subthalamic network [9]. Therefore, the location in the network can be assessed clinically as well as using measurements of physiological signals.

Examples of non-motor acute behavioral phenomena elicited by stimulation abound, such as euphoria, involuntary smiles, hypomania, and others, usually identified as side effects of stimulation or indicative of placement in an undesired area [10–14]. Unlike the well-characterized motor changes that are correlated with electrophysiological readouts, these behaviors have not been described along with physiological correlates in clinical settings. In SCC DBS, our group reported on the findings of intraoperative behavior and its relation to the contact locations within the network impacted by stimulation [8]. The most commonly observed intraoperative behaviors involved a rapid change in patients’ interoceptive awareness. These stereotypical responses included: “feeling lighter, calmer”, “more awake, aware, and reactive”, suggestive of acute autonomic activation. These responses were denoted “Type 1”. A second overlapping set of responses, designated as “Type 2”, involved not only the interoceptive awareness, but also an increased sense of exteroceptive awakening. Patients reported feeling more connected with the outside world. These responses were unequivocal and reproducible for each subject in the operating room.

The present study sought to examine the physiological readouts of these intraoperative responses to SCC stimulation, and their association with the anatomical substrates that generated them. We measured autonomic reactivity during a testing session performed during SCC DBS surgery, using measures of heart rate and electrodermal activity. Additionally, we related these physiological surrogates of intraoperative response to structural connectivity patterns of subcallosal cingulate stimulation mediating *acute* intraoperative behavior responses with the goal to identify an intraoperative biomarker of optimal SCC lead placement. We hypothesized that subjective behavioral responses would co-occur with an increase in autonomic arousal, specific to the location of stimulation. We expected these changes would be associated with the structural connectivity from the stimulated area to regions involved in autonomic control. An understanding of these circuits may help dissect this complex syndrome into several circuit-based components, lending the possibility of matching certain behavioral and physiologic domains to specific networks [15,16].

Methods

Participants

Nine consecutive ($M(SD)_{\text{age}} = 46.22(8.29)$, 7 female) patients with severe, chronic, treatment-resistant major depressive disorder were enrolled in a research protocol at Emory University to test the safety and efficacy of SCC DBS (clinicaltrials.gov NCT00367003). The protocol was approved by the Institutional Review Board at Emory University and by the US Food and Drug Administration under Investigational Device Exemption G060028 sponsored by one of us (H.S.M.) and is monitored by the Data and Safety Monitoring Board of the Department of Psychiatry and Behavioral Sciences, Emory University. All participants signed an informed consent to participate; all patients continue in the ongoing longitudinal study. Further information regarding clinical outcomes was published [7].

The study inclusion and exclusion criteria were identical to those previously published by Holtzheimer et al. [17]. In brief, patients had a depressive episode of at least one year duration, a Hamilton Depression Rating Scale severity score of 20 or higher; trials of at least 4 antidepressant treatments (including electroconvulsive therapy) without improvement; no significant psychiatric or medical comorbidities; and significant functional impairment with a Global Assessment of Function score of less than 50 (range, 1–100, with higher scores indicating better function).

DBS implantation surgery

Procedure

The surgical procedure for DBS lead and pulse generator implantation followed published methods [17]. Targeting in these participants was chosen using a tractography-based connectomics prospective method [7]. Target, localization of the DBS lead tip, and trajectory were done using a surgical planning workstation (StealthStation S7, Medtronic Inc, Louisville, CO). Bilateral DBS leads (Libra system, St Jude Medical, Plano, TX), each with 4 contacts (1.5 mm inter-contact spacing) were inserted and secured and with the patient awake and alert for testing initiated thereafter.

Intraoperative behavior response assessments

The stimulation protocol consisted of 12 trials (one at each of the 8 available contacts; 4 per hemisphere, plus 4 sham trials) of 3 minutes with stimulation, followed by 3 min without stimulation. Testing utilized standard parameters for chronic SCC stimulation (single contact, monopolar stimulation delivered with St Jude Medical External Neurostimulator with current return path to patient's shoulder, frequency = 130 Hz, pulse width = 90 μsec, current = 6 mA). The order of active or ‘sham’ trials was randomized with both subject and the clinician rater blinded to the condition. In one case, only the patient was blinded. No post hoc blinding assessments were conducted, and the stimulation was delivered from behind the surgical drapes to avoid involuntary unblinding of the rater. The “3 min ON/3 min OFF” design maximized the likelihood of adequate time to capture both acute (within the first minute) and sustained (maintained throughout the stimulation epoch) behavioral changes as well as to ensure that a new baseline was reestablished prior to the subsequent trial. Patients were instructed to report any changes in sensation, feelings, mood or thought and to describe any changes when queried. Self-reports were recorded at fixed time points within each trial (after 1 minute from initiation of stimulation). After surgery, responses for each of the stimulation trials were reviewed and categorized. When the stimulation elicited an intraoperative response, features were further classified into two categorical ‘types’ based on the salience, quality and magnitude of the self-report. The subjects reported in this study, as well as their subjective intraoperative responses, are the same as those described in Choi et al. [8]. Response Type 1 was defined by presence solely of a perceived change in body state (i.e., interoceptive awareness), or specific physical sensations. Response Type 2 was characterized by a more complex set of evoked thoughts and feelings commonly indicated by a shift in attention from themselves to others (exteroceptive awareness). Once rankings were completed, trials were unblinded and contacts (Left 1–4; Right 1–4) were matched to trial and response types. These classifications were subsequently used for psychophysiological and structural connectivity analyses.

Psychophysiological measures

Time-locked changes in heart rate and skin conductance were recorded during each stimulation cycle. Stimulation was time-locked with the recordings. The facial EMG recordings detect the initiation and presence of electrical stimulation. The onset of stimulation was precisely identified for each stimulation period. An event marker was placed for each sham stimulation on the psychophysiological recordings during the intraoperative testing. Seven patients had electrocardiogram (ECG) data and five patients had skin conductance data that were adequate for processing and analysis. All psychophysiological recordings were acquired on a BIOPAC MP100 (Biopac Inc., Goleta, CA) for 4 patients and MP150 for 5 patients. One patient was excluded from the analysis because the quality of their psychophysiology data was inadequate.

Heart Rate. Electrocardiogram (ECG) data was recorded with a lead III configuration. The continuous heart rate in beats per minute (BPM) was calculated using rate calculation of the ECG channel in Biopac Acqknowledge 4.1. Artifacts in heart rate channel were manually removed through linear interpolation across the artifact-affected heart rate data. Average HR was calculated for the 3-min stimulation periods as a whole and separately, in 15-s windows across the stimulation epochs. Change in HR was calculated by subtracting the average 15-s pre-stimulus baseline from each stimulation epoch.

Skin Conductance. Electrodermal activity (EDA) was recorded from both hands simultaneously. For all analyses, data from the hand with the fewest artifacts was used. All artifacts in the EDA channel were linearly interpolated. The maximum trough-to-peak change in SCR amplitude was derived across each stimulation period. All SCR measurements were square root transformed to adjust for typical skew in the SCR amplitude distribution and to make the distribution more normal [18,19].

Image acquisition and processing

All MR imaging data was collected within a single session for each subject on Siemens 3 T Tim-Trio scanner (Siemens Medical Solution, PA. USA) including high-resolution T1 and diffusion weighted images. FSL software toolbox (FMRIB software Library, http://www.fmrib.ox.ac.uk/fsl) was used for preprocessing. A post-surgical high-resolution computer tomography (CT) image was acquired on a LightSpeed16 (GE Medical System) with resolution $0.46 \times 0.46 \times 0.65\ \text{mm}^3$. Detailed image acquisition parameters and pre-processing steps are described in previously published paper by Choi et al. [8].

Computational modeling of volume of tissue activated (VTA)

The patient-specific DBS VTA was generated by using the electrical DBS field model method [20]. Based on the electrode and contact locations that were identified using post-surgical CT images, the VTA for each contact was generated using a DBS neurosurgical research software [21] with following stimulation parameters: 130 Hz, 90 μs, and 6 mA [22]. All VTAs were transferred to the MNI152 template using a combination of linear and nonlinear registrations.

Structural connectivity analysis

Ten regions of interest (ROIs) were selected from cortical and subcortical brain regions based on previous structural and

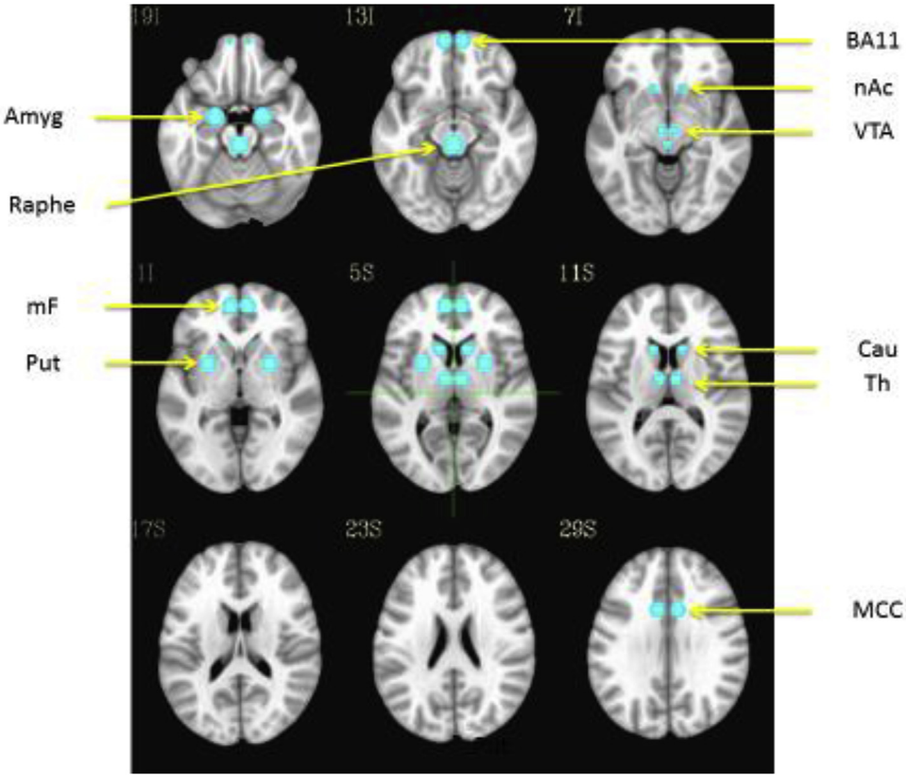

Fig. 1. Illustrations of structural connectivity targets (ROIs). Probabilistic tractography between these 10 individual ROIs and the volume of tissue activated were generated in FSL (with a CSF stop mask). Amyg: Amygdala; Raphe: Raphe Nucleus; mF: medial frontal (BA10); Put: Putamen; BA11: Brodmann's Area 11 (anterior medial frontal); nAc: nucleus accumbens; VTA: Ventral Tegmental Area; Cau: Caudate; Th: Thalamus; MCC: Mid-Cingulate Cortex.

functional connectivity findings and known white matter bundle involvement for SCC DBS [6,23–25]. These ROIs include the mid-cingulate (MCC), medial frontal (mF), amygdala, caudate, putamen, thalamus, nucleus accumbens (nAc), orbitofrontal cortex, raphe nuclei, and ventral tegmental area bilaterally (Fig. 1). Probabilistic tractography between patient-specific VTAs and pre-defined target ROIs was performed using the Fdt toolbox (FSL) with following parameters: 5000 samples per seed voxel, a curvature threshold of 0.2, a step length of 0.5, and a maximum number of steps of 2000. Using a seed-to-target method in Probtrackx2 toolbox (FSL), the connectivity value from each VTA to target ROIs was computed. The connectivity value between VTA and target was normalized by the total number of sample tracts generated from VTA [26]. The normalized connectivity value was later correlated with psychophysiological measurements such as heart rate and skin conductance change with active stimulation.

Statistics

All statistical analyses were performed in SPSS 23 (IBM Corporation, North Castle, NY). A planned comparison (paired *t*-test) was performed to test the hypothesis that heart rate would increase for stimulation conditions relative to sham conditions. One-way repeated measures ANOVAs were performed on averages across the data calculated from the whole stimulation cycles relative to sham cycles. For repeated measures ANOVAs, we subtracted the effect of sham on heart rate from the heart rate effect for each behavioral category to account for any effects on heart rate during sham conditions. All data were normally distributed based on a Kolmogorov−Smirnov (K-S Test) of normality. No outliers were detected using a ± 2 standard deviations approach. Post-hoc comparisons using paired-samples t-tests was used to test for differences between behavioral response types and sham stimulation. Paired t-tests across each behavioral response type at each time

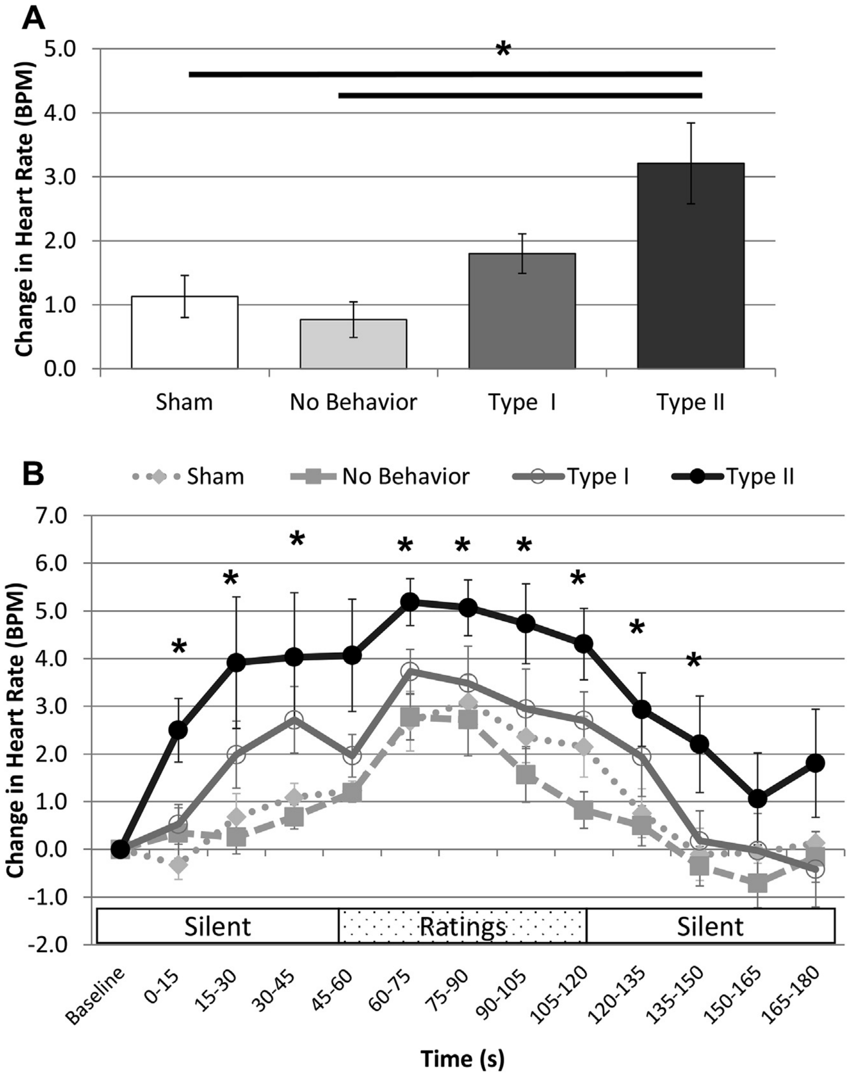

Fig. 2. Change in Heart Rate from SCC DBS by behavioral type and hemisphere. Intraoperative DBS to the locations in the SCC gray/white matter border produce an increase in heart rate as a function of the type of subjective behavioral response elicited and the hemisphere of stimulation for each monopolar contact stimulated. A) Average maximum change in heart rate across 3 min of SCC DBS from a 15 s pre-stimulus baseline by type of subjective behavioral response. B) Time course in 15 s increments of heart rate change to SCC DBS across 1 min of silence, 1 min of ratings, and another minute of silence as a function of behavioral response type. Heart rate acutely increases during the first 15 s of stimulation that produces a Type II behavioral response and remains elevated for the duration of stimulation. C) Average maximum change in heart rate across 3 min of SCC DBS from a 15 s pre-stimulus baseline by presence of a behavioral response and hemisphere of stimulation. Left SCC stimulation that produced a behavioral response elicited increases in heart rate across the entire stimulation period relative to right SCC stimulation, stimulation conditions with no behavioral change, and sham stimulation. D) Time course in 15 s increments of heart rate change to SCC DBS across 3 min of stimulation as a function of the presence of a behavioral response and hemisphere of stimulation. Left SCC stimulation that produced a behavioral response elicited an acute and sustained increase in heart rate relative to right SCC stimulation that produced a behavior, no behavior, and sham stimulation conditions. $^*p < 0.05$.

point were also performed on the change in HR data to examine when the autonomic response to SCC DBS was the greatest for each behavioral response type. Finally, to examine the relationship of the number of estimated streamlines emanating from the VTA in the SCC to each tract of the SCC DBS network and changes in heart rate a correlation was performed on each patient's data for each hemisphere of stimulation. The r-value for each trial was then standardized with a Fisher's Z transformation so that the correlations of HR change and white matter connectivity to the SCC could be averaged across patients. This average of Fisher's Z scores across patients was then submitted to a one-way ANOVA comparing the average correlation to zero for each VTA tract (i.e., SCC to dorsal anterior cingulate, medial frontal, and nucleus accumbens). Following review, only ROIs that had connectivity were included in the correlation analysis to changes in heart rate.

Results

First, we examined the effects of SCC DBS on the change in heart rate for sham versus all stimulation trials using a paired *t*-test to test for the overall effect of stimulation relative to sham. A one-way ANOVA revealed an overall increase in heart rate for stimulation trials relative to sham trials, $f(1,6) = 6.26$, $p = 0.04$, $\eta_p^2 = 0.51$. Then, we examined the effects of SCC DBS on the change in heart rate for each behavioral response condition (no behavior, Type 1, and Type 2 responses) relative to sham using a one-way ANOVA to test for omnibus effects of SCC DBS and post-hoc t-tests to examine differences between specific conditions. To account for any effects on heart rate during sham conditions, we subtracted the effect of sham on heart rate from the heart rate effect for each behavioral category. A one-way repeated measures ANOVA showed an effect of stimulation ($f(2,6) = 7.2$, $p = 0.009$, $\eta_p^2 = 0.54$), with SCC DBS to the most behaviorally salient contacts (Type 2 responses) causing a significant increase in HR relative to non-behaviorally effective contacts and sham ($t(6) = 4.3$, $p = 0.005$, $d = 1.64$; Fig. 2A). Type 1 behavioral responses did not show a significant increase in HR relative to non-behaviorally effective contacts and sham ($t(6) = 2.2$, $p = 0.07$, $d = 0.83$). The autonomic changes were observed within seconds of initiating acute stimulation and prior to verbalization of subjective experiences. In time window analyses, paired t-tests revealed that Type 2 responses produced a significant increase in the initial 15 second time period relative to sham ($t(6) = 4.17$, $p = 0.006$, $d = 1.57$), non-behaviorally effective ($t(6) = 5.2$, $p = 0.002$, $d = 1.96$), and Type 1 responses ($t(6) = 3.15$, $p = 0.02$, $d = 1.19$). For the rest of the time windows, except the 45–60 s and 150–180 s time windows, SCC stimulation trials that produced a behavioral response (Type 1 or Type 2) were significantly different from sham and non-behaviorally effective trials (all $p < 0.05$; Fig. 2B).

Second, we examined the effects of SCC DBS on the change in heart rate for behaviorally effective and non-effective conditions in the left and right hemispheres relative to sham conditions. An one-way ANOVA showed an effect of stimulation ($f(2,6) = 7.02$, $p = 0.01$, $\eta_p^2 = 0.54$), with SCC DBS to the behaviorally effective, left hemisphere stimulation causing a significant increase in HR relative to non-effective conditions ($t(6) = 4.93$, $p = 0.003$, $d = 1.86$) and to sham ($t(6) = 4.82$, $p = 0.003$, $d = 1.82$; Fig. 2C). Right hemisphere trials that produced behavioral responses did not show a significant increase in HR relative to non-behaviorally effective contacts and sham. In time window analyses, paired t-tests revealed that left SCC DBS that led to any behavioral responses produced a significant increase in the initial 15-s time period relative to non-behaviorally effective ($t(6) = 2.55$, $p = 0.04$, $d = 0.96$), sham ($t(6) = 3.15$, $p = 0.02$, $d = 1.18$), and behaviorally effective, right hemisphere stimulation ($t(6) = 2.55$, $p = 0.04$, $d = 0.96$). For time windows between zero to 45 s, and between 60 and 150 s of stimulation, SCC stimulation trials that produced any behavioral response (Type 1 or Type 2) on the left were significantly different from sham and non-behaviorally effective trials ($p < 0.05$; Fig. 2D).

Third, we estimated structural connectivity between the ipsilateral SCC DBS volume of tissue activated (VTA) to four of 10 network node targets in each hemisphere known to be associated with the antidepressant effects of SCC DBS (Mid-Cingulate Cortex, Brodmann's Area 11, Medial Frontal Cortex, and Nucleus Accumbens). Consistent structural connectivity estimations were not

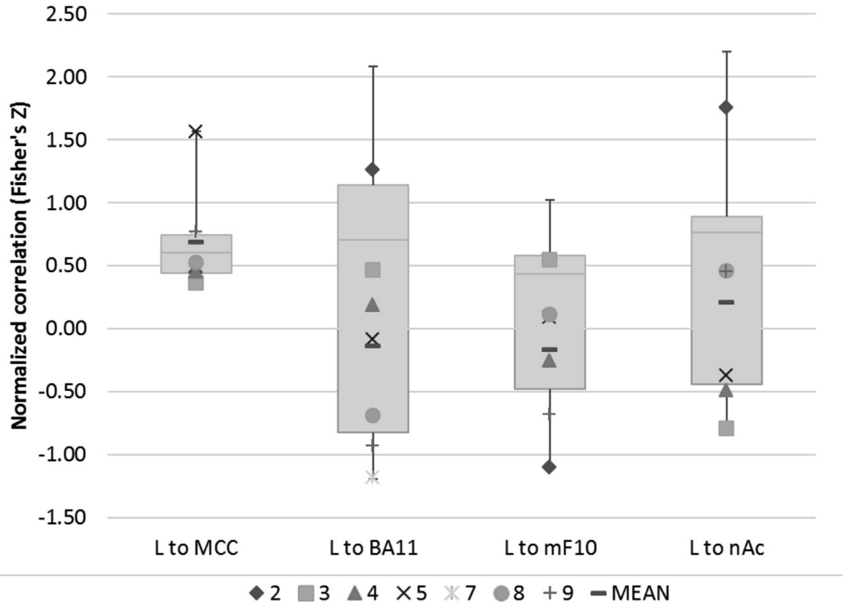

Fig. 3. Heart rate change is correlated with the number of streamlines between left SCC volume of tissue activated and the left mid-cingulate cortex (*). There were no significant findings in the correlation between Left SCC to BA11, mF10 or nAc. Normalized correlation (Fisher's Z) for each subject of the change in heart rate with left SCC stimulation and normalized DTI connectivity from SCC to distinct ROIs in the DBS network. * = $p < 0.05$. MCC = Mid Cingulate Cortex, BA11 = Brodmann's Area 11, mF10 = Medial Frontal Cortex, BA10, nAc = Nucleus Accumbens. Symbols indicate data from individual patients.

found for the other 6 network node targets (Amygdala, Raphe Nucleus, Ventral Tegmental Area, Caudate, Thalamus, Putamen), and were thus not analyzed further. The normalized connectivity values from each VTA to target ROIs were not significantly different in the left and right hemispheres (all $p > 0.05$). Correlations between these estimates of structural connectivity and physiological changes in heart rate were derived for each patient and then normalized for group comparison using a Fisher's Z transformation. Each patient's normalized correlation was submitted to a one-sample *t*-test (comparing against a Fisher's Z of 0). Across all 7 patients, we found a significant relationship between the estimated structural connectivity of the left SCC VTA to the mid-cingulate cortex and the change in heart rate for stimulation of each SCC electrode. Specifically, we found that the greater the structural connectivity between the SCC VTA and the mid-cingulate cortex, the more the heart rate increased for that specific stimulation trial ($t(6) = 4.18$, $p = 0.006$, $d = 1.57$; Fig. 3). Estimated structural connectivity SCC VTA for the left and right hemisphere targets did not significantly differ from one another ($ps > 0.05$). We found no significant relationships between the estimated structural connectivity of the SCC VTA to any other potential connected targets and the change in heart rate ($p\text{'s} > 0.05$).

Finally, we examined the effects of SCC DBS on electrodermal activity or skin conductance responses (SCR). These results are limited due to a small sample size and low power given that only 5 patients had valid intraoperative SCR recordings. Similar to the results for heart rate, we found that the magnitude of SCRs was greater for Type 2 responses and left SCC stimulation that produced any behavioral response than for sham and non-effective stimulation conditions, but these findings did not reach statistical significance. Most subjects had large increases in SCR that were time-locked to the onset of stimulation (Fig. 4).

Discussion

This study has established relationships between three variables that have previously only been described independently. These include the existence of clinically relevant intraoperative behaviors, the presence of autonomic reactivity with electrical intracranial SCC stimulation, and the requirement to precisely modulate a

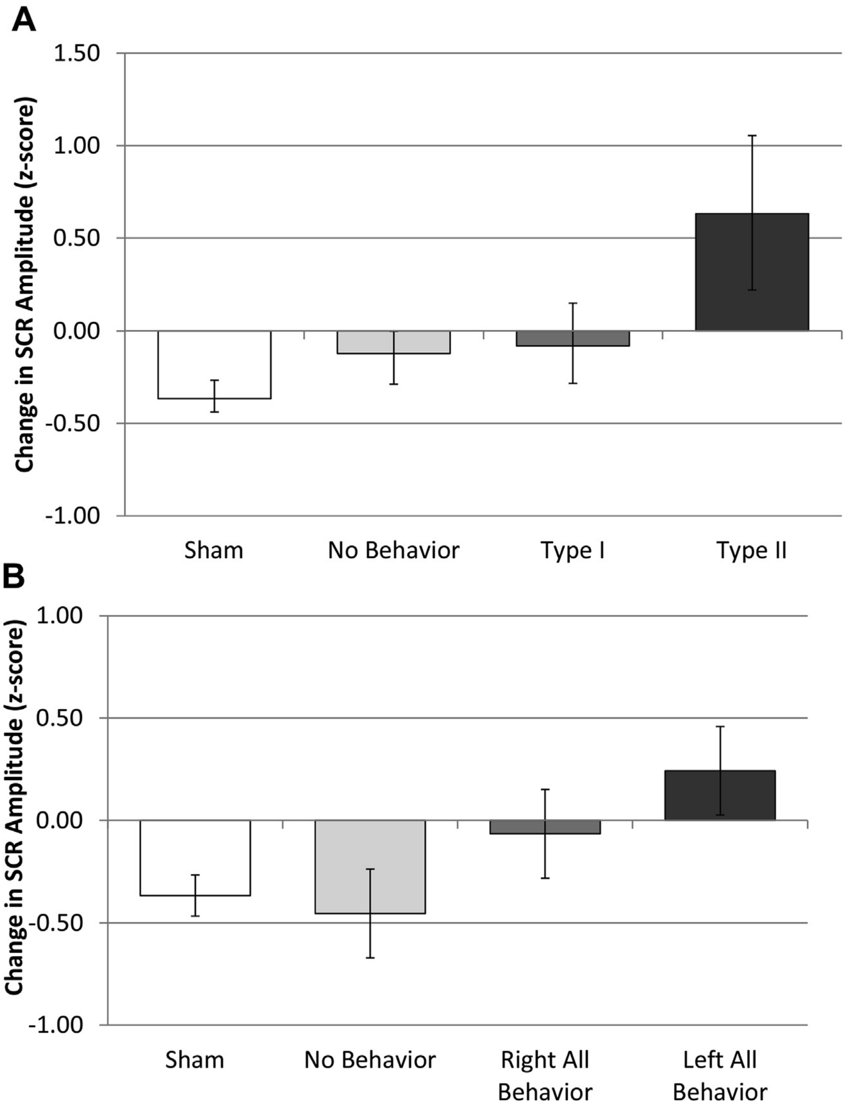

Fig. 4. Change in normalized skin conductance amplitude from SCC DBS by behavioral type (panel A) and by hemisphere (panel B). A) Average maximum change in normalized skin conductance across 3 min of SCC DBS by type of subjective behavioral response. Normalized skin conductance amplitude was increased for Type 2 behavioral responses relative to Type 2, no behavior, and sham conditions. B) Average maximum change in normalized skin conductance across 3 min of SCC DBS by presence of a behavioral response and hemisphere of stimulation.

specific network for acute antidepressant effects. Here we established the relationships between each variable (Fig. 5). Intraoperative SCC stimulation produces increases in autonomic response that correspond with the type of behavioral response. Specifically, SCC DBS generates increases in sympathetic activity relative to sham stimulation, indicated by changes in heart rate. Changes were observed within seconds of initiating acute stimulation and before verbalization of subjective experiences. Particularly, stimulation generating the most behaviorally salient responses (Type 2) were associated with the greatest increases in heart rate (HR). Further, left hemispheric stimulation caused a significantly higher increase in HR than sham, while right SCC stimulation did not. Our group previously described the relationship between stimulation of the necessary white matter network and intraoperative behaviors [8]. In this study, we further demonstrated that the white matter between the stimulated area and the midcingulate is the potential pathway mediating autonomic responsivity to SCC DBS. Interestingly, structural connectivity from left SCC to left midcingulate cortex (MCC) was the only connection positively correlated with the increases in HR (Fig. 3). Therefore, SCC stimulation produces autonomic and behavioral changes intraoperatively that are explained by the modulation of networks associated with long-term antidepressant response.

Across the entire testing period, stimulation causing Type 2 responses elicited the largest HR increases. Type 2 responses have a distinct physiological response relative to all other conditions that were apparent in the initial 15 s of stimulation, providing an objective measure to differentiate Type 2 responses from other conditions. Type 1 responses also had HR increases, albeit only numerically greater than sham. Contacts generating Type 2 responses were later selected for effective chronic stimulation in the left hemisphere. The observation of the HR changes occurring in the initial time windows (0–45 s) is most notable. Here, patients were asked to be silent and there were no interviewer prompts, avoiding confounding factors that influence sympathetic reactivity. Not only did the most behaviorally effective contacts cause an immediate HR increase, but these periods showed a sustained elevation in HR that was maintained through each epoch. Changes in sympathetic activity were strongly correlated with the most behaviorally salient periods. These findings confirm with physiologic readouts that SCC DBS modulates distant areas involved in autonomic regulation, providing an objective measure of target identification [27].

The present study supports the idea that structural connectivity between SCC and midcingulate cortex (MCC) provides a conduit for autonomic reactivity regulation during intraoperative stimulation. Measurements of white matter connectivity between SCC and other regions involved in chronic DBS antidepressant response (mF10 and 11, nucleus accumbens, subcortical areas) did not show a relationship with measurements of autonomic reactivity. The normalized connectivity of the left and right SCC to the target ROIs are similar, and HR increases most with left SCC stimulation, suggesting that autonomic components of SCC DBS response may be lateralized to the left MCC. Reports of white matter disruption in the cingulum bundle have shown lack of autonomic reactivity, and patients with prior cingulotomies do not have changes in autonomic reactivity with intraoperative subcaudate stimulation [28]. This suggests that intact connections between ACC and MCC are required to have salient behavioral responses and autonomic reactivity to stimulation. Other groups have described related findings with neuroimaging [29]. A recent meta-analysis of 43 fMRI and PET studies showed that MCC is one of the core centers for the central autonomic processing [30]. The MCC and the dorsal anterior cingulate cortex (dACC) are important in the generation of autonomic arousal accompanying volitional cognitive behavior in fMRI. Direct electrical stimulation of the SCC may bypass the volitional component. Activity in dorsal anterior/midcingulate cortices correlates with sympathetic cardiovascular influences [31]. Functional imaging in patients with DBS reported that, despite local SCC changes observed in all participants, only the responders to DBS had remote changes in the dorsal ACC [5]. This emphasizes the need for network modulation and a “connectomics approach” to DBS, describing the remote activation of areas within the network.

The broader significance of this work points to several novel insights about autonomic and behavioral effects of SCC DBS. Beyond well-described subjective behavioral responses there is a need for objective measures of target identification such as

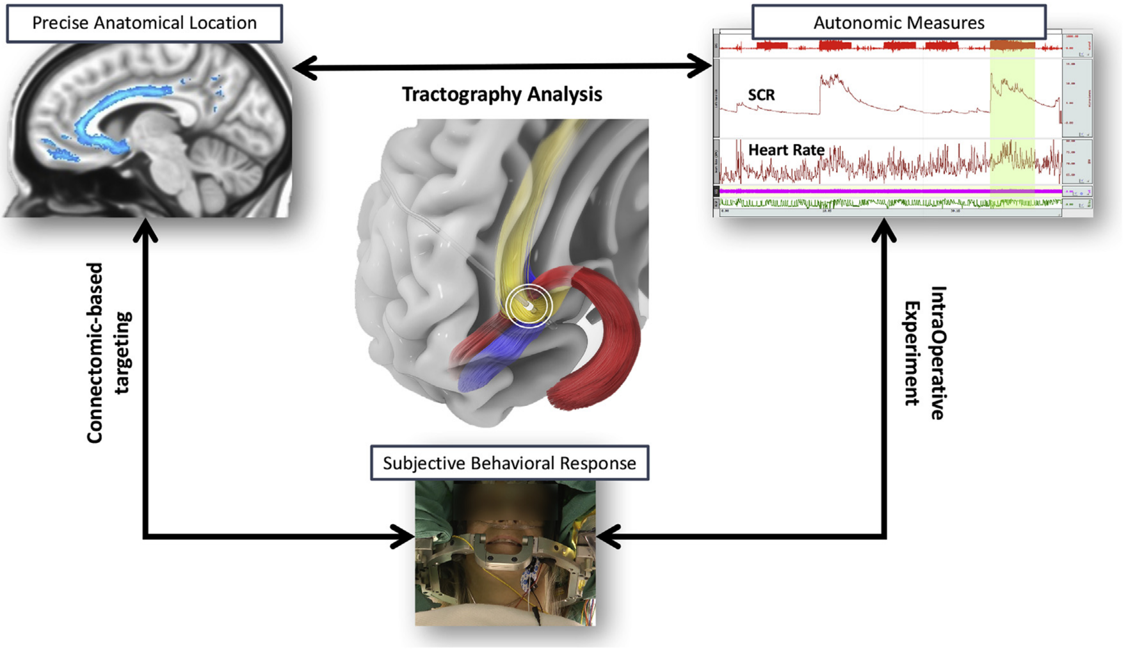

Fig. 5. Model of intraoperative autonomic and subjective responses based on prospectively planned DTI SCC targeting.

measurements of central or peripheral activity related to SCC stimulation. Our study provides one necessary objective measure of target identification with the HR changes seen during acute stimulation of precise SCC white matter nodes. However, these measures are not sufficient to capture the full acute antidepressant effect. The breadth of the antidepressant effects described intraoperatively include descriptions that exceed a purely autonomic explanation. Despite this limitation, autonomic responses usefully allow for intraoperative distinctions to be made between effective and non-effective stimulation locations, and subjective responses to sham stimulation. Further, the distinct readouts of autonomic reactivity in this study are evidence of the distant effects that SCC DBS generates in the network, and more precisely in its connections to the MCC as compared to the other linked regions that are connected to the SCC, like the frontal medial lobes. Our conclusions are in line with the described role of the MCC in autonomic control. Identification of reliable biomarkers is a necessary step in the refinement and development of advanced DBS technologies. Similarly to the use of electrophysiology in movement disorders, these biomarkers may aid in the confirmation of adequate placement and stimulation parameters during surgery [32]. Future studies recording the intrinsic neuronal activity of this region and other regions connected to the SCC will shed light on the each of the nodes' roles in the antidepressant effects [33,34]. Overall, intraoperative autonomic recordings paired with careful behavioral observations and precise anatomical mapping aid in the identification and classification of the intraoperative phenomena.

The study has a number of limitations. First, the classification of behaviors observed with acute stimulation into distinct categories has been previously described but relies on clinical interpretation of subjective responses. Behavioral responses have multiple potential confounds such as pain, fatigue, or discomfort that patients experience during awake intraoperative testing. While these responses could be misinterpreted, the objective measures of autonomic peripheral activity provide support for distinction between different behavioral responses. Second, although the intraoperative environment was as controlled as possible for autonomic recordings, it is not the best setting for sensitive recordings. The sham stimulation conditions controlled for the environmental confounds. Testing of these measures in an extraoperative environment will allow for clearer autonomic data examining parameters of electrical stimulation (location, amplitude, frequency) with improved quality of EDA, blood pressure, pupillary reactivity, and facial expression changes. Third, DBS delivered with standard, non-steerable, leads does not allow for modulation of specific white matter fibers, i.e. isolated forceps minor or cingulum bundle. Forth, larger sample sizes will be needed to more thoroughly test the effect of SCC DBS on changes in autonomic activity, like electrodermal activity. Fourth, the possibilities of stimulation parameters are extensive, and this study did not explore the entire parameter space in terms of current, frequency or pulse width. It is entirely possible that different settings could produce different sets of intraoperative responses. Future studies should explore a larger portion of the parameter space outside of the intraoperative environment given its time and logistical limitations. Finally, the connectivity between regions in the network that do not travel through the SCC was not analyzed. Thus, we could not see whether a direct connection between the left medial frontal region and the MCC could explain the Type 2 responses. These white matter pathways have been well described in human and non-human primates [35]. Although white matter connectivity measured with DTI is sensitive to measuring primary pathways passing through a region of interest [6] and has been effective in selecting patient-specific SCC DBS stimulation targets [7], estimating connectivity for smaller pathways passing through the SCC might require more robust DTI measures of white matter connectivity.

These physiological findings may have applications in optimizing SCC DBS surgery, aiding in the selection of contacts and the stimulation settings that will impact specific neural networks. Further, changes in sympathetic activity with SCC DBS provide a novel strategy for examining the interactions of affective experience and the autonomic nervous system in TRD. The findings of objective autonomic measures that are seen in selected contacts allow for better explanation of the intraoperative behavioral and autonomic effects. Our prior work described the precision of surgical targeting and the predicted intraoperative responses [8]. With this report, we can "close the loop" and find the basis of behavioral manifestations in autonomic measures as well as the selective network stimulation when the combination of autonomic measures and tractography are considered.

Patricio Riva-Posse, Cory Inman, KiSueng Choi, Andrea Crowell and Stephan Hamann have no conflicts of interest. Robert E. Gross has received grants from Medtronic Inc., Neuropace and MRI Interventions, honoraria from Medtronic Inc. and MRI Interventions; and is a paid consultant to St Jude Medical Corp., Medtronic Inc., Neuropace, MRI Interventions, Neuralstem and SanBio. These arrangements were approved by Emory University. Dr. Helen Mayberg is an unpaid consultant with licensed intellectual property to St Jude Medical Corp (now Abbott Labs).

Acknowledgements

We would like to thank the patients and Mayberg lab staff. This work was supported by the Hope for Depression Research Foundation.

References

[1] Ressler KJ, Mayberg HS. Targeting abnormal neural circuits in mood and anxiety disorders: from the laboratory to the clinic. Nat Neurosci 2007;10(9):1116–24.
[2] Malone Jr DA, Dougherty DD, Rezai AR, Carpenter LL, Friehs GM, Eskandar EN, et al. Deep brain stimulation of the ventral capsule/ventral striatum for treatment-resistant depression. Biol Psychiatry 2009;65(4):267–75.
[3] Bewernick BH, Hurlemann R, Matusch A, Kayser S, Grubert C, Hadrysiewicz B, et al. Nucleus accumbens deep brain stimulation decreases ratings of depression and anxiety in treatment-resistant depression. Biol Psychiatry 2010;67(2):110–6.
[4] Schlaepfer TE, Bewernick BH, Kayser S, Madler B, Coenen VA. Rapid effects of deep brain stimulation for treatment-resistant major depression. Biol Psychiatry 2013;73(12):1204–12.
[5] Mayberg HS, Lozano AM, Voon V, McNeely HE, Seminowicz D, Hamani C, et al. Deep brain stimulation for treatment-resistant depression. Neuron 2005;45(5):651–60.
[6] Riva-Posse P, Choi KS, Holtzheimer PE, McIntyre CC, Gross RE, Chaturvedi A, et al. Defining critical white matter pathways mediating successful subcallosal cingulate deep brain stimulation for treatment-resistant depression. Biol Psychiatry 2014;76(12):963–9.
[7] Riva-Posse P, Choi KS, Holtzheimer PE, Crowell AL, Garlow SJ, Rajendra JK, et al. A connectomic approach for subcallosal cingulate deep brain stimulation surgery: prospective targeting in treatment-resistant depression. Mol Psychiatr 2018 Apr;23(4):843–9. https://doi.org/10.1038/mp.2017.59. Epub 2017 Apr 11. PMID: 28397839.
[8] Choi KS, Riva-Posse P, Gross RE, Mayberg HS. Mapping the "depression switch" during intraoperative testing of subcallosal cingulate deep brain stimulation. JAMA neurology 2015;72(11):1252–60.
[9] Wingeier B, Tcheng T, Koop MM, Hill BC, Heit G, Bronte-Stewart HM. Intra-operative STN DBS attenuates the prominent beta rhythm in the STN in Parkinson's disease. Exp Neurol 2006;197(1):244–51.
[10] Okun MS, Bowers D, Springer U, Shapira NA, Malone D, Rezai AR, et al. What's in a "smile?" Intra-operative observations of contralateral smiles induced by deep brain stimulation. Neurocase 2004;10(4):271–9.
[11] Bejjani BP, Damier P, Arnulf I, Thivard L, Bonnet AM, Dormont D, et al. Transient acute depression induced by high-frequency deep-brain stimulation. N Engl J Med 1999;340(19):1476–80.
[12] Bejjani BP, Houeto JL, Hariz M, Yelnik J, Mesnage V, Bonnet AM, et al. Aggressive behavior induced by intraoperative stimulation in the triangle of sano. Neurology 2002;59(9):1425–7.

[13] Shapira NA, Okun MS, Wint D, Foote KD, Byars JA, Bowers D, et al. Panic and fear induced by deep brain stimulation. J Neurol Neurosurg Psychiatr 2006;77(3):410–2.

[14] Hamani C, McAndrews MP, Cohn M, Oh M, Zumsteg D, Shapiro CM, et al. Memory enhancement induced by hypothalamic/fornix deep brain stimulation. Ann Neurol 2008;63(1):119–23.

[15] Wiens S. Interoception in emotional experience. Curr Opin Neurol 2005;18(4):442–7.

[16] Craig AD. Interoception: the sense of the physiological condition of the body. Curr Opin Neurobiol 2003;13(4):500–5.

[17] Holtzheimer PE, Kelley ME, Gross RE, Filkowski MM, Garlow SJ, Barrocas A, et al. Subcallosal cingulate deep brain stimulation for treatment-resistant unipolar and bipolar depression. Arch Gen Psychiatr 2012;69(2):150–8.

[18] Boucsein W. Electrodermal activity. second ed. Springer; 2012.

[19] Dawson ME, Schell AM, Filion DL. The electrodermal system. Handbook of psychophysiology, 2; 2007. p. 200–23.

[20] Chaturvedi A, Lujan JL, McIntyre CC. Artificial neural network based characterization of the volume of tissue activated during deep brain stimulation. J Neural Eng 2013;10(5):056023.

[21] Noecker AM, Choi KS, Riva-Posse P, Gross RE, Mayberg HS, McIntyre CC. StimVision software: examples and applications in subcallosal cingulate deep brain stimulation for depression. Neuromodulation 2018 Feb;21(2):191–6. https://doi.org/10.1111/ner.12625. Epub 2017 Jun 27. PMID: 28653482.

[22] Lujan JL, Chaturvedi A, Choi KS, Holtzheimer PE, Gross RE, Mayberg HS, et al. Tractography-activation models applied to subcallosal cingulate deep brain stimulation. Brain Stimul. 2013;6(5):737–9.

[23] Johansen-Berg H, Gutman DA, Behrens TE, Matthews PM, Rushworth MF, Katz E, et al. Anatomical connectivity of the subgenual cingulate region targeted with deep brain stimulation for treatment-resistant depression. Cerebr Cortex 2008;18(6):1374–83.

[24] Gutman DA, Holtzheimer PE, Behrens TE, Johansen-Berg H, Mayberg HS. A tractography analysis of two deep brain stimulation white matter targets for depression. Biol Psychiatry 2009;65(4):276–82.

[25] Dunlop BW, Rajendra JK, Craighead WE, Kelley ME, McGrath CL, Choi KS, et al. Functional connectivity of the subcallosal cingulate cortex and differential outcomes to treatment with cognitive-behavioral therapy or antidepressant medication for major depressive disorder. Am J Psychiatry 2017;174(6):533–45.

[26] Li L, Rilling JK, Preuss TM, Glasser MF, Hu X. The effects of connection reconstruction method on the interregional connectivity of brain networks via diffusion tractography. Hum Brain Mapp 2012;33(8):1894–913.

[27] Paus T, Koski L, Caramanos Z, Westbury C. Regional differences in the effects of task difficulty and motor output on blood flow response in the human anterior cingulate cortex: a review of 107 PET activation studies. Neuroreport 1998;9(9):R37–47.

[28] Gentil AF, Eskandar EN, Marci CD, Evans KC, Dougherty DD. Physiological responses to brain stimulation during limbic surgery: further evidence of anterior cingulate modulation of autonomic arousal. Biol Psychiatry 2009;66(7):695–701.

[29] Critchley HD, Mathias CJ, Dolan RJ. Neuroanatomical basis for first- and second-order representations of bodily states. Nat Neurosci 2001;4(2):207–12.

[30] Beissner F, Meissner K, Bär K-J, Napadow V. The autonomic brain: an activation likelihood estimation meta-analysis for central processing of autonomic function. J Neurosci 2013;33(25):10503–11.

[31] Critchley HD, Mathias CJ, Josephs O, O'Doherty J, Zanini S, Dewar BK, et al. Human cingulate cortex and autonomic control: converging neuroimaging and clinical evidence. Brain J Neurol 2003;126(Pt 10):2139–52.

[32] Widge AS, Malone Jr DA, Dougherty DD. Closing the loop on deep brain stimulation for treatment-resistant depression. Front Neurosci 2018;12:175.

[33] Lo MC, Widge AS. Closed-loop neuromodulation systems: next-generation treatments for psychiatric illness. Int Rev Psychiatr 2017;29(2):191–204.

[34] Smart O, Choi KS, Riva-Posse P, Tiruvadi V, Rajendra J, Waters AC, et al. Initial unilateral exposure to deep brain stimulation in treatment-resistant depression patients alters spectral power in the subcallosal cingulate. Front Comput Neurosci 2018;12:43.

[35] Petrides M, Pandya DN. Efferent association pathways from the rostral prefrontal cortex in the macaque monkey. J Neurosci Off. J Soc Neurosci 2007;27(43):11573–86.